

Second harmonic generation at thin film silver electrodes via surface polaritons

Robert M. Corn,^{a)} Marco Romagnoli, Marc D. Levenson, and Michael R. Philpott
IBM Research Laboratory, San Jose, California 95193

(Received 14 May 1984; accepted 29 June 1984)

The generation of second harmonic light from a silver–mica capacitor and from thin film silver electrodes provides information on the charge and composition of the metal–dielectric interface. The second harmonic light is created by the injection of surface polaritons onto the electrode surface via prism coupling techniques. A theory relating the second harmonic intensity to the square of the charge on the electrode successfully predicts the dependence of the SHG on applied voltage or potential and the time dependence of the SHG in response to a potential step. The time dependent second harmonic signal is also used to monitor the growth of a lead monolayer onto the silver electrode in the region of underpotential deposition.

I. INTRODUCTION

Optical studies of electrodes enhance our understanding of electrochemistry by probing the structure and the reactivity of the electrochemical interface. The emergence of the fields of spectroelectrochemistry, surface-enhanced Raman scattering (SERS), and surface infrared spectroscopy at electrodes attests to the success of these methods in complementing the traditional current-voltage measurements on electrochemical systems. One optical technique which has proved to be very useful in examining surfaces (electrochemical and otherwise) is the nonlinear optical process of second harmonic generation (SHG). SHG from the interface between two centrosymmetric media is uniquely sensitive to the surface region, and has been employed at solid–vacuum,¹ solid–gas,² and solid–liquid³ interfaces. The second harmonic light from the surface is unperturbed by the propagation through the adjacent bulk phases, and can be collected with a very modest amount of instrumentation. In general, studies of the nonresonant SHG can yield information on the electronic structure of the surface, and resonant SHG can provide molecular details about the interface.

Recently we reported the use of surface polaritons at thin film silver electrodes to measure the potential dependence of the nonresonant SHG from the electrochemical interface.⁴ We found that to a first approximation the second harmonic intensity was proportional to the square of the charge density on the electrode, and as such was sensitive to changes in solution and surface composition. Although SHG from electrochemical surfaces was first examined some time ago,⁵ the surface sensitivity of the technique has only recently generated interest in this nonlinear process.^{6–8} However, the electrochemical studies to date have focused on roughened interfaces, where SHG has been used to help quantify the electric field enhancement provided by those surfaces.⁸ The roughened surfaces employed in those studies, however, as well as the roughened surfaces required for SERS, are difficult to reproduce, sensitive to photoinduced changes in morphology⁹ and in general do not lend themselves readily to quantitative study.

We have avoided these difficulties by using surface polaritons to generate second harmonic light at a metal surface. Surface polaritons are well-characterized electromagnetic waves which provide us with a quantifiable amount of electric field enhancement at a reproducible (vacuum-deposited) silver surface. Surface polaritons have also been employed in this lab¹⁰ and elsewhere^{11,12} to produce enhanced Raman scattering and fluorescence from molecules near a silver surface.

This paper details our further studies on SHG from thin film electrodes via surface polaritons. Our experiments illustrate how the charge density on the electrode can be monitored by the second harmonic intensity under steady-state conditions or as a function of time, in the presence of adsorption and charging currents, and during Faradaic processes.

We first present a brief theoretical introduction into how surface polaritons are used to produce SHG, and then outline the phenomenological theory which describes SHG from an electrified interface. Using this theory we then analyze the potential dependence of the second harmonic signal from a silver–mica capacitor and from a thin film silver electrode in a solution of 0.1 M sodium sulfate. We find that as a first approximation the SHG from the surface follows the square of the excess charge density. This finding is further substantiated by the time dependence of the SHG in response to a potential step. And finally, we show how SHG can be used to monitor Faradaic reactions at electrodes by measuring the time dependence of the SHG as a monolayer of lead is deposited from solution onto the silver film during the process of underpotential deposition (upd).

II. THEORY

A. SHG via plasmon surface polaritons at a metal–dielectric interface

Plasmon surface polaritons (PSPs) are the coupled surface electromagnetic modes of photons and the surface plasmon excitations of a metal which, in our case, is silver. Classically, these electromagnetic waves propagate parallel to the silver surface with an electric field amplitude that decays exponentially into the two media:

$$E(\omega, t) = E_0(\hat{x} + ik_x \hat{z}/\alpha_1) e^{-\alpha_1 z} e^{i(k_x x - \omega t)}, \quad z > 0, \quad (1)$$

$$E(\omega, t) = E_0(\hat{x} - ik_x \hat{z}/\alpha_2) e^{\alpha_2 z} e^{i(k_x x - \omega t)}, \quad z < 0, \quad (2)$$

^{a)} Present address: Department of Chemistry, Swarthmore College, Swarthmore, PA 19081.

where we have set the x - y plane at $z = 0$ onto the surface of the silver ($z < 0$) and are looking at a PSP at frequency ω propagating in the positive x direction with wave vector k_x . To first order the surface polaritons are linearly TM polarized in the z direction (since $k_x/\alpha_i \gg 1$). As shown in Eqs. (1) and (2), the exponential decay into the two adjacent media need not be symmetric; for a PSP at 532 nm on a silver-water interface $1/\alpha_2$ is 23 nm for the silver and $1/\alpha_1$ is 160 nm for the water. In general, the penetration depth $1/\alpha_i$ depends on the dielectric constants and the PSP wave vector by Eq. (3):

$$\alpha_i^2 = k_x^2 - \epsilon_i \omega^2 / c^2, \quad i = 1, 2. \quad (3)$$

As alluded to in Eq. (3), the wave vector k_x is not equal to the wave vector of a photon of corresponding frequency in the dielectric. In general the PSP wave vector obeys the dispersion relation

$$1 + \alpha_1 \epsilon_2 / \alpha_2 \epsilon_1 = 0. \quad (4)$$

This dispersion relation is plotted in Fig. 1 for PSPs at a silver-water interface. As shown in the figure, the wave vector for the PSP is larger than the free photon wave vector for all frequencies below the surface plasmon cutoff frequency ω_{sp} (above ω_{sp} the PSPs are strongly damped by absorption in the silver film). Thus, due to the conservation of momentum, one cannot create PSPs on an isolated metal surface. This difficulty is surmounted by using a thin film of metal and coupling through to the opposite side. This technique of attenuated total reflection (ATR)¹³ is what we have employed to launch PSPs onto the electrode surface; further discussion of the technique can be found in Ref. 4. The net result of the ATR method is that in order for the incident light from the laser beam on the back side of the silver film to create a PSP on the opposite surface its wave vector must have the same x component as that of a PSP with the same frequency. This "plasmon angle matching" leads to a specific requirement on the input angle θ_ω and is shown schematically with the wave vectors in Fig. 2.

Second harmonic light would be created on the surface

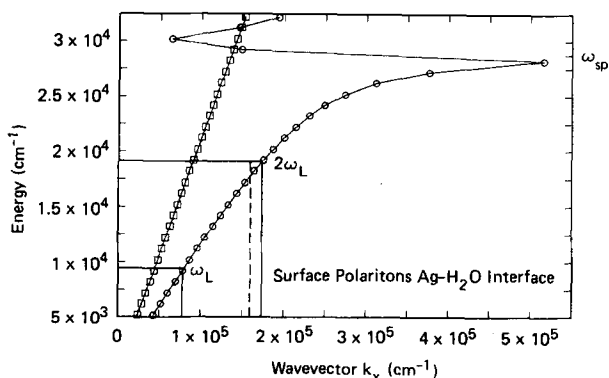


FIG. 1. The effect of PSP dispersion on SHG at a silver-water interface. The circles are the calculation of the dependence of the frequency ω on the wave vector k_x for a PSP on the surface. No PSPs exist above the surface plasmon cutoff frequency ω_{sp} . At very low frequencies, k_x approaches the value of a wave vector for a free photon in bulk water (denoted by the squares). Depicted in the figure with solid lines are the particular wave vectors for PSPs at the fundamental frequency ω_L ($\lambda = 1060$ nm) and the second harmonic frequency $2\omega_L$ ($\lambda = 532$ nm). Since SHG is a coherent process, PSPs at frequency 2ω are inaccessible and only reflected photons with a wave vector whose x component is equal to $2k_x(\omega)$ (dashed line) are created.

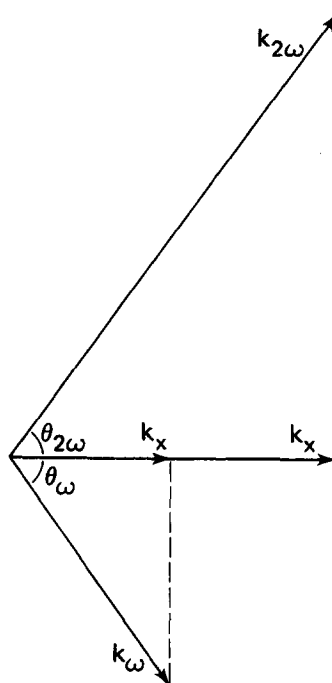


FIG. 2. Wave vector diagram for SHG at a surface via PSPs. The x component of the wave vector k_ω for the incident light must be equal to the wave vector k_x for the PSPs on the surface; this requirement leads to the plasmon matching angle θ_ω . Generation of photons with wave vector $k_{2\omega}$ will occur only at the angle $\theta_{2\omega}$, where the x component of the wave vector is equal to $2k_x$, due to the phase-matching conditions required for the coherent process of SHG.

from the injected PSPs in the most efficient manner if a new PSP could be produced at frequency 2ω and subsequently coupled back out through the prism at the corresponding plasmon angle. Unfortunately, since SHG is a coherent process it also requires phase matching of the initial and final wave vectors. This phase matching requirement cannot be fulfilled with PSPs due to nature of their dispersion curve; no PSPs exist with frequency 2ω and wave vector $2k_x$ (see Fig. 1). Instead, we observe the creation of reflected photons which have a wave vector whose x component is equal to twice that of the PSP wave vector at frequency ω . This simultaneous plasmon and phase matching of the light is drawn vectorially in Fig. 2, showing how these conditions lead to specific input and output angles for the fundamental and second harmonic beams. These angles have been calculated for our samples⁴ and are found to agree with the experimentally observed angles to within 1° .

B. SHG from an electrified interface

As shown in earlier studies, SHG from an electrified interface arises from the sum of a dc field independent nonlinear polarization P_0 and a dc field dependent nonlinear polarization P_1 ^{5,8}:

$$P_0(2\omega) = \alpha E(\omega) \times H(\omega) + \beta [\nabla \cdot E(\omega)] E(\omega) + (\delta - \beta) [E(\omega) \cdot \nabla] E(\omega) + \chi^{(2)} : E(\omega) : E(\omega), \quad (5)$$

$$P_1(2\omega) = \gamma E_{dc} |E(\omega)|^2 + \gamma' E(\omega) [E_{dc} \cdot E(\omega)], \quad (6)$$

where the first three terms on the right-hand side of Eq. (5) correspond to the SHG at the surface due to the magnetic dipole and electric quadrupole contributions to the SHG, and the fourth term is from any noncentrosymmetric material present at the interface (e.g., adsorbates). The overall second harmonic signal $I_{2\omega}$ is proportional to the square of the vector sum of the two, which in our case [with E_{dc} and $E(\omega)$ perpendicular to the surface] is

$$I_{2\omega} \propto a + b(E_{dc} + c)^2, \quad (7)$$

where the constants a , b , and c are given by $|\text{Im } P_0|^2$, $(\gamma + \gamma')|\mathbf{E}(\omega)|^2$, and $\text{Re } P_0/b$, respectively (we have assumed γ, γ' real). If we view the silver to first order as a perfect conductor then the static electric field should be proportional to the surface charge density σ :

$$I_{2\omega} \propto a + b \left(\frac{4\pi\sigma}{\epsilon_1(0)} + c \right)^2. \quad (8)$$

We shall use Eq. (8) to relate the second harmonic intensity to the amount of excess charge density on the silver surface. Theoretical studies^{14,15} using a hydrodynamic model for the metal electrons also suggest that the surface currents responsible for the SHG from surfaces should depend directly upon the amount of excess charge at the interface.

C. Time dependence of the second harmonic signal

We will wish to examine the time dependent response of the second harmonic signal to a potential step at the electrode. This response can arise from two factors: (i) a change in the charge density on the electrode, and (ii) a change in the optical constants in Eq. (8) due to a modification of the electrode surface by electrodeposition. The first process, the change in the charge density after a potential step, is well documented and has been studied extensively with chronoamperometry¹⁶: the charge density on the electrode as a function of time is given by

$$\sigma(t) = \sigma_f + (\sigma_i - \sigma_f)e^{-t/\tau}, \quad (9)$$

where σ_i is the charge on the electrode at the initial potential, σ_f is the charge on the electrode at the final potential, and τ is the time constant for the electrochemical cell. The time constant τ is equal to the product of the electrode capacitance and the uncompensated resistance of the solution; we have assumed that the capacitance is independent of electrode potential. Using Eqs. (8) and (9) the time response of the second harmonic signal is straightforward:

$$I_{2\omega} \propto \frac{16\pi^2 b}{\epsilon_1(0)} [\sigma_f + (\sigma_i - \sigma_f)e^{-t/\tau}]^2. \quad (10)$$

We have neglected the constant c in determining the time dependence in Eq. (10) because we shall find that it is small in the systems which we are examining (see below).

The second method for altering the second harmonic signal from the interface is to affect a Faradaic reaction with the potential step, electrodepositing material onto the electrode and changing the optical constants of the surface. We will be monitoring the underpotential deposition of a monolayer of lead onto a silver electrode. In general, underpotential deposition is a multistep process,¹⁷ but if the electrochemical reaction is very fast then the time dependence becomes controlled by the diffusion of the reactant(s) to the electrode surface. The diffusion to a planar electrode is governed by Fick's law and leads to a time dependent surface concentration of reactant $\Gamma(t)$ which is given approximately by Eq. (11)¹⁸:

$$\Gamma(t) = 2\pi^{-1/2} D^{1/2} C_0 t^{1/2}, \quad (11)$$

where D is the diffusion constant and C_0 is the bulk concentration of the reactant. From Eq. (11) we can get an estimate of the time scale for diffusion of a monolayer of lead to the

electrode surface; by choosing a Γ of $+5 \times 10^{-10}$ mol-cm⁻², the approximate surface concentration for a close packed layer of lead atoms (radius = 1.75 Å), a diffusion constant of 0.5×10^{-5} cm² s⁻¹, and a bulk concentration of 5×10^{-6} mol cm⁻³ we calculate an approximate time constant of 20 ms. Thus, we should see the SHG from the surface change on that time scale. On the other hand, if the formation of the Pb metal is kinetically controlled by a surface process, we would expect the second harmonic signal to change more gradually.

III. EXPERIMENTAL CONSIDERATIONS

All of the experiments utilized the fundamental beam of a Q -switched Quanta-Ray DCR Nd:YAG laser at 1060 nm to create second harmonic light at 532 nm. The laser has a pulse width of 15 ns in Q -switched operation and was modified to have a homogeneous output beam. In order to avoid laser irradiation damage to the samples the repetition rate was set at 2 Hz and the energy density of the unfocused beam was kept at or below 2 mJ/cm².

The first experiment onto which the beam was directed consisted of a hemicylindrical prism of high index of refraction glass (Schott SF5, $n = 1.65$ at 1060 nm) which was pressed with index-matching fluid onto a large capacitor consisting of a sandwich of 45 nm of silver, 35 μ m of ruby mica, and 200 nm of silver. The silver films were deposited onto the mica in vacuum with their thickness being monitored by a quartz microbalance. The angle of incidence for the laser beam was that required for injection of PSPs onto the silver-mica interface as calculated from Fresnel's equations and was verified by the observation of a strong minimum in the reflected fundamental beam.

The entire sample was mounted onto a double rotary table which allowed not only for the adjustment of the input but also for the selection of the proper output angle for the second harmonic beam. This second harmonic light was detected with an RCA C31034 photomultiplier tube: the enhancement from the PSPs was sufficient to allow for the signal to be read directly off an oscilloscope.

For the electrochemical measurements a 45 nm silver film was deposited directly onto the SF5 prism which was then pressed onto an electrochemical cell that has been described previously.⁴ The silver film then became the working electrode for a standard Princeton Applied Research (PAR) model 173 three electrode potentiostat, which allows for the measurement of potential of the working electrode and current passed through the working electrode. For our experiments a Ag/AgCl reference electrode was employed to define the potential, and a Pt wire completed the three electrode arrangement. Reagent grade sodium sulfate, Alfa Products "Puratronic Grade" sodium acetate and lead acetate and deionized water were used in preparing the electrolyte solutions. All solutions were thoroughly deoxygenated with argon prior to injection into the sealed electrochemical cell. For the potential step experiments a 10 to 100 ms potential step of 100 to 500 mV was applied to the electrochemical cell by a PAR 175 pulse programmer (via the PAR 173) in synchronization with the laser pulse at a repetition rate of approximately 2 Hz. The laser pulse was then delayed a

varying amount with respect to the potential step in order to monitor the time dependence of the SHG from the electrode.

IV. RESULTS AND DISCUSSION

A. SHG from a silver–mica capacitor

In order to get a quantitative measure of the dependence of SHG from an electrified interface on the applied voltage we prepared a silver–mica capacitor in which one electrode was a thin silver film onto which we could create PSPs. The ruby mica dielectric was chosen for its high breakdown voltage, but it also happens to be a noncentrosymmetric crystal and will therefore generate additional second harmonic light via the $\chi^{(2)}$ term in Eq. (5). To ascertain the effects of the additional signal we also prepared a capacitor using mylar as the dielectric material (which, being amorphous, is centrosymmetric).

Equation (7) predicts a second harmonic signal which is quadratic with the applied voltage, and whose minimum should be shifted from the zero in the electric field. Figure 3 plots the square root of the signal vs the voltage applied to the capacitor. As predicted by Eq. (7), we observe a minimum in the potential at a nonzero applied voltage; this voltage corresponds to an electric field strength of -6.6×10^6 V/cm. The minimum in the mylar capacitor experiment was shifted to -3.6×10^5 V/cm. The smaller shift is expected since the constant c in Eq. (7) is proportional to the nonlinear polarization P_0 . Both of these shifts occur at fields approximately one to two orders of magnitude less than those expected at the electrochemical interface.¹⁹ We therefore expect to observe only a small shift in the second harmonic response from the electrochemical systems.

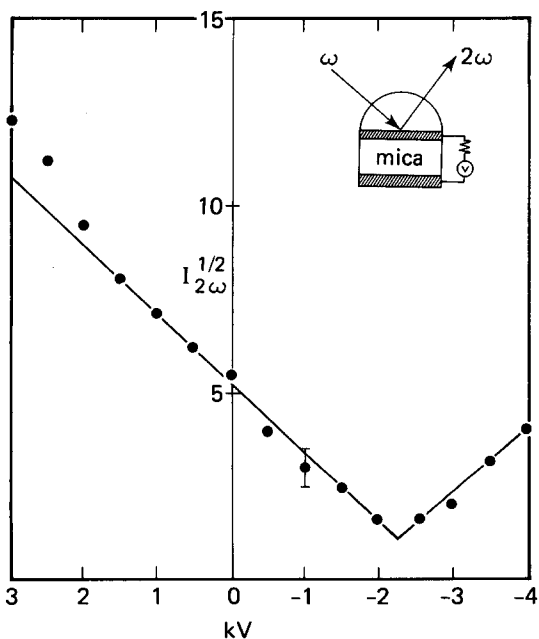


FIG. 3. SHG from a silver–mica capacitor. Light at 532 nm is generated from a Nd:YAG laser pulse at 1060 nm via the creation of PSPs at the silver–mica interface (see inset). The square root of the second harmonic intensity $I_{2\omega}$ is plotted as a function of voltage applied to the capacitor. An applied voltage of 1 kV corresponds to an electric field strength of 2.86×10^5 V/cm.

B. SHG from a silver electrode in contact with 0.1 M sodium sulfate

SHG from a silver electrode shows similar but not identical properties to that from the capacitor. The square root of the SHG from a thin silver film in contact with an aqueous solution of 0.1 M sodium sulfate is plotted as a function of electrode potential (relative to Ag/AgCl) in Fig. 4. Sodium sulfate was chosen as a supporting electrolyte for its nonadsorbing characteristics; adsorption of anions onto the electrode surface has been found to affect the potential dependence of the SHG.⁴ Similar curves to that shown in Fig. 4 have been obtained for an electrolyte of sodium perchlorate (also nonadsorbing), and in the presence of an organic adsorbate (urea).⁴

We observe a minimum in the SHG from the electrode at -750 mV vs Ag/AgCl. As reported in Ref. 4, the vacuum deposited films used in the experiments were found from x-ray diffraction measurements to be polycrystalline with approximately 90% of the crystallites oriented with their (111) surfaces parallel to the substrate. From careful differential capacitance measurements on Ag (111) electrodes the potential of zero charge (pzc) for the Ag (111) surface has been placed at -735 mV vs Ag/AgCl.²⁰ This is very close to the minimum we observe in our second harmonic measurements, and this small observed shift is in agreement with calculations which predict the magnitude of the electric field at an electrode to be on the order of 10^7 to 10^8 V/cm.¹⁹ Thus we find that the hyperpolarizability terms (P_1) dominate the second harmonic signal from the electrochemical systems, and we can neglect the constant c in Eq. (7).

A major difference in the second harmonic response of the electrochemical system as compared to the capacitor is the deviation from the quadratic dependence of the signal on the applied potential. This deviation is responsible for the

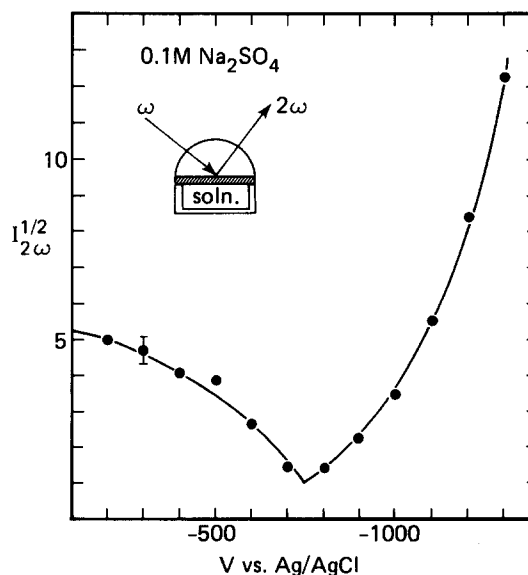


FIG. 4. SHG from a silver electrode in contact with a 0.1 M Na_2SO_4 solution. PSPs are created on a thin film silver electrode and second harmonic light is generated at the silver–electrolyte interface. The square root of the second harmonic intensity is plotted as a function of electrode potential; the approximate potential of zero charge for the silver film is at -735 mV vs Ag/AgCl.

curvature in the second harmonic potential dependence plotted in Fig. 4, and is due to two reasons. The first is our gross assumption that the charge on the electrode varies linearly with applied potential (from our assumption of a potential-independent capacitance). In general this is not the case, and measurements on Ag (111) electrodes do show deviations from linearity.²⁰ The second reason for the nonquadratic dependence of the second harmonic intensity on applied potential is the very large fields that are present at the electrochemical interface. These fields require the inclusion of higher order terms than the linear hyperpolarizability in Eq. (5), which, in turn, lead to potential dependent optical constants in Eq. (8). The breakdown of Eq. (8) will also create deviations from the predicted time dependence of the second harmonic signal [Eq. (9)].

C. Response of the second harmonic signal to a potential step

As outlined above, when a potential step is applied to an electrochemical cell, the charging current to the electrode does not respond immediately, but rather with a characteristic time constant given by the product of the solution resistance and the electrode capacitance. By taking advantage of the time resolution afforded us with the pulsed Nd:YAG laser we can monitor changes in the second harmonic signal from the electrode by delaying the laser pulse with respect to the potential step. The results of such an experiment are plotted in Fig. 5. In the first case (open circles) the potential was stepped from a place where the charge was virtually zero (-750 mV) to a potential where there was a substantial amount of charge on the electrode (-1250 mV). The second experiment (solid circles) was the reverse step. At the same time we measured the charging currents delivered to the electrode and calculated from those measurements a time constant of 5 ms. Using Eq. (9) we then calculated the time

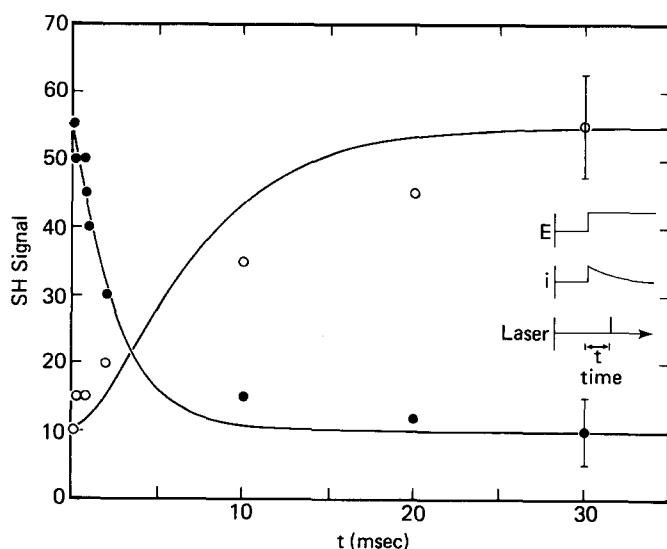


FIG. 5. Time response of the SHG from a silver electrode to a potential step. The second harmonic signal after a time t from a potential step is measured by delaying the laser pulse (see inset). Two experiments are plotted; in the first the potential was stepped from -750 to -1250 mV (open circles), and in the second the reverse step was performed (solid circles). The solid lines are the theoretical curves calculated from Eq. (10) with a time constant τ of 5 ms as measured from the current transient from the electrode. The electrolyte is 0.1 M Na_2SO_4 .

response of the SHG and plotted it along with the data in Fig. 5. The theoretical curves fit reasonably well considering the approximations made in the theory. In particular, the curvature of the potential curves mentioned in the previous section should cause significant deviations from the theory based on Eq. (7). But, to a first approximation, we can still consider the SHG to follow the square of the charge on the electrode.

D. Second harmonic signal during the deposition of a monolayer of lead

As a final experiment we used the ability to measure the time dependence of the second harmonic signal to study a Faradaic process, the underpotential deposition of a monolayer of lead. Electrochemical and reflectance measurements²¹ have shown that prior to the bulk deposition of Pb^{2+} ions from solution a monolayer of lead is deposited onto the surface of a silver electrode (upd). In Ref. 4 we showed that the SHG from a silver electrode dramatically decreased in the region where upd had occurred. By stepping from a potential where there is no lead on the surface (-250 mV) to a point in this region (-450 mV) we can monitor the loss of second harmonic signal and the formation of the monolayer of lead. The results plotted in Fig. 6 reveal that there are three mechanisms for the loss of second harmonic intensity. At short times (< 50 ms) we see a loss in second harmonic intensity due to (i) the change in charge on the electrode as observed in the previous experiment, and (ii) the adsorption of Pb^{2+} ions, which we calculated above to occur in this time region (both processes are required to account for the total loss of second harmonic signal that was observed). After 50 ms we see a loss of SHG from the surface on a longer time scale; we assume this loss is due to the formation of the metal from the adsorbed Pb^{2+} ions. Experiments on the current transients from similar potential step measurements²¹ indicate that the Faradaic currents associated with the formation of the metal monolayer also occur on the same time scale. Thus, we see that the time response of the second harmonic intensity depends on a combination of electrode processes: charging currents and adsorption processes on a short time scale and surface kinetics on a longer time scale.

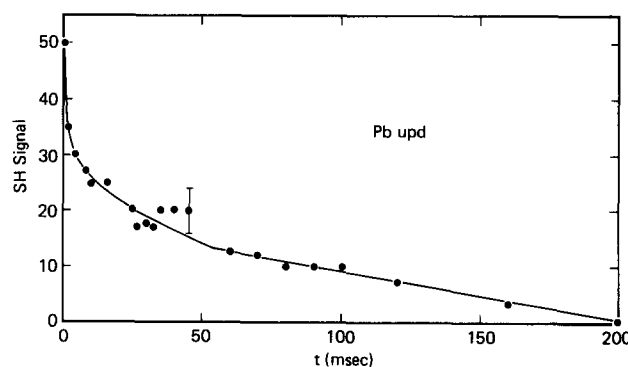


FIG. 6. Time dependence of SHG during underpotential deposition of a monolayer of lead. A potential step from -250 to -450 mV in a solution of 0.1 M sodium acetate + 5 mM lead acetate forms a monolayer of lead on the silver electrode surface. The decrease in SHG as a function of time shows a short time behavior (< 50 ms) due to charging and adsorption processes, and a long time behavior (> 50 ms) due to the surface kinetics of the formation of the lead monolayer.

V. SUMMARY AND CONCLUSIONS

The above experiments illustrate how the second harmonic signal can be a useful tool in studying the structure and reactivity of electrochemical interfaces. We are now able to directly measure the charge on an electrode on a very rapid time scale, and in the presence of other electrode processes such as adsorption and charge transfer. Through the use of plasmon surface polaritons we are able to generate large amounts of second harmonic intensity without the need for preroughening of the electrode surface, a process which obscures the electrode processes and greatly complicates the interfacial chemistry. The simple theory outlined in Sec. II relating the SHG to the square of the charge density on the surface is sufficient to explain the second harmonic intensity during a number of electrode processes as a function of time and potential. We expect in the future that the SHG will be used to help elucidate the mechanisms of very fast electrode processes such as photochemical dye sensitization of electrodes and electron transfer reactions.

ACKNOWLEDGMENTS

In conclusion we would like to thank J. G. Gordon II, D. Buttry, and O. Melroy for many helpful discussions and to J. Escobar and G. Borges for their technical support. This work was supported in part by the Office of Naval Research.

- ¹H. W. K. Tom, C. M. Mate, J. E. Crowell, T. F. Heinz, G. A. Somorjai, and Y. R. Shen, *Phys. Rev. Lett.* **52**, 348 (1984).
- ²N. Bloembergen, R. K. Chang, S. S. Jha, and C. H. Lee, *Phys. Rev.* **174**, 813 (1968).
- ³C. C. Wang, *Phys. Rev.* **178**, 1457 (1969).
- ⁴R. M. Corn, M. Romagnoli, M. D. Levenson, and M. R. Philpott, *Chem. Phys. Lett.* **106**, 30 (1984).
- ⁵C. H. Lee, R. K. Chang, and N. Bloembergen, *Phys. Rev. Lett.* **18**, 167 (1967).
- ⁶C. K. Chen, A. R. B. de Castro, and Y. R. Shen, *Phys. Rev. Lett.* **46**, 145 (1981).
- ⁷C. K. Chen, T. F. Heinz, D. Ricard, and Y. R. Shen, *Phys. Rev. Lett.* **46**, 1010 (1981).
- ⁸C. K. Chen, T. F. Heinz, D. Ricard, and Y. R. Shen, *Phys. Rev. B* **27**, 1965 (1983).
- ⁹D. V. Murphy, K. U. von Raben, T. T. Chen, J. F. Owen, R. K. Chang, and B. L. Laube, *Surf. Sci.* **124**, 529 (1983).
- ¹⁰R. M. Corn and M. R. Philpott, *J. Chem. Phys.* **80**, 5245 (1984).
- ¹¹S. Ushioda and Y. Sasaki, *Phys. Rev. B* **27**, 1401 (1982).
- ¹²R. Dornhaus, R. E. Benner, R. K. Chang, and I. Chabay, *Surf. Sci.* **101**, 367 (1980).
- ¹³E. Kretschmann and H. Raether, *Z. Naturforsch. Teil A* **23**, 2135 (1968).
- ¹⁴J. Rudnick and E. A. Stern, in *Polaritons*, edited by E. Burstein and F. DeMartini (Plenum, New York, 1974).
- ¹⁵J. E. Sipe, V. C. Y. So, M. Fukui, and G. I. Stegeman, *Phys. Rev. B* **21**, 4389 (1980).
- ¹⁶See, for example, A. J. Bard and L. R. Faulkner, *Electrochemical Methods* (Wiley, New York, 1980).
- ¹⁷D. M. Kolb, in *Advances in Electrochemistry and Electrochemical Engineering*, edited by H. Gerischer and C. W. Tobias (Wiley, New York, 1978), Vol. 11.
- ¹⁸P. Delahay and I. Trachtenberg, *J. Am. Chem. Soc.* **79**, 2355 (1957).
- ¹⁹See, for example, J. O'M. Bockris and A. K. N. Reddy, *Modern Electrochemistry* (Plenum, New York, 1970), Vol. 2.
- ²⁰G. Vallete and A. Hamelin, *J. Electroanal. Chem.* **45**, 301 (1973).
- ²¹A. Bewick and B. Thomas, *J. Electroanal. Chem.* **84**, 127 (1977).